Short-term heat stress altered metabolism and insulin signaling in skeletal muscle

Shanthi Ganesan,[*] Corey M. Summers,[*,†] Sarah C. Pearce,[*] Nicholas K. Gabler,[*] Rudy J. Valentine,[†] Lance H. Baumgard,[*] Robert P. Rhoads,[‡] and Joshua T. Selsby[*,1]

[*]Department of Animal Science, Iowa State University, Ames, IA 50011; [†]Department of Kinesiology, Iowa State University, Ames, IA 50011; and [‡]Department of Animal and Poultry Sciences, Virginia Tech, Blacksburg, VA 24061

ABSTRACT: Heat-related complications continue to be a major health concern for humans and animals and lead to potentially life-threatening conditions. Heat stress (**HS**) alters metabolic parameters and may alter glucose metabolism and insulin signaling. Therefore, the purpose of this investigation was to determine the extent to which 12 h of HS-altered energetic metabolism in oxidative skeletal muscle. To address this, crossbred gilts (n = 8/group) were assigned to one of three environmental treatments for 12 h: thermoneutral (**TN**; 21 °C), HS (37 °C), or pair-fed to HS counterparts but housed in TN conditions (**PFTN**). Following treatment, animals were euthanized and the semitendinosus red (**STR**) was recovered. Despite increased relative protein abundance of the insulin receptor, insulin receptor substrate (**IRS1**) phosphorylation was increased (P = 0.0005) at S307, an inhibitory site, and phosphorylated protein kinase B (**AKT**) (S473) was decreased (P = 0.03) likely serving to impair insulin signaling following 12 h of HS. Further, HS increased phosphorylated protein kinase C (**PKC**) ζ/λ (P = 0.02) and phosphorylated PKCδ/θ protein abundance (P = 0.02), which are known to regulate inhibitory serine phosphorylation of IRS1 (S307). Sarcolemmal glucose transporter 4 (**Glut4**) was decreased (P = 0.04) in the membrane fraction of HS skeletal muscle suggesting diminished glucose uptake capacity. HS-mediated increases (P = 0.04) in mechanistic target of rapamycin (**mTOR**) were not accompanied by phosphorylation of eukaryotic translation initiation factor 4E-binding protein 1 (**4EBP1**). HS decreased (P = 0.0006) glycogen synthase (**GS**) and increased (P = 0.02) phosphorylated GS suggesting impaired glycogen synthesis. In addition, HS altered fatty acid metabolic signaling by increasing (P = 0.02) Acetyl-CoA carboxylase (**ACC**), decreasing (P = 0.005) phosphorylated ATP-citrate lyase (**pATPCL**) and fatty acid synthase (P = 0.01) (**FAS**). These data suggest that 12 h of HS blunted insulin signaling, decreased protein synthesis, and altered glycogen and fatty acid metabolism.

Key words: fatty acid, heat stress, insulin, protein metabolism, skeletal muscle, swine

J. Anim. Sci. 2018.96:154–167
doi: 10.1093/jas/skx083

INTRODUCTION

Heat stress (**HS**) negatively impacts livestock production by limiting efficient animal growth and it also jeopardizes animal welfare (St-Pierre et al., 2003; Baumgard and Rhoads, 2013). Though cooling is the primary treatment for HS (Vicario et al., 1986; Johnson et al., 2016), it does not treat underlying pathological mechanisms. Thus, understanding HS-mediated cellular changes is important.

HS negatively impacts mitochondrial function (Addabbo et al., 2009), induces mitochondrial damage (Caspani et al., 2004), and compromises efficient ATP production. Further,

This work was supported by USDA grants 2014-67015-21627 (JTS) and 2011-6700330007 (LHB). The authors thank ISU-Genome Informatics Facility and MRL lab for technical assistance.

[1]Corresponding author: jselsby@iastate.edu

Received January 5, 2017.
Accepted February 6, 2018.

HS decreased protein accretion and increases lipid deposition (Geraert et al., 1996; Temim et al., 2000; Collin et al., 2001) despite reduced caloric intake, suggesting energetically atypical alterations to nutrient partitioning (Baumgard and Rhoads, 2013). Moreover, HS increased glycolytic rates, evidenced by increased lactate production and pyruvate kinase activity in HS broiler muscle (Zhang et al., 2012).

Of interest, prolonged HS (>24 h) increases basal and circulating insulin and decreases adipose tissue mobilization in a variety of species (Baumgard and Rhoads, 2013; Sanz Fernandez et al., 2015a, 2015b). The effects of HS on circulating glucose concentrations are less consistent; reduced in some instances (Becker et al., 1992; Shwartz et al., 2009) and increased in others (Prunier et al., 1997; Pearce et al., 2013). Recent studies indicate 12 h of HS decreased circulating insulin and increased nonesterified fatty acid (**NEFA**) without altering blood glucose concomitant (Pearce et al., 2015b) with evidence of mitochondrial dysfunction (Ganesan et al., 2017), and increased inflammatory signaling (Ganesan et al., 2016). Importantly, the impact of a shorter duration of HS (12 h) on metabolic signaling in skeletal muscle is unknown. Thus, we hypothesize that HS will alter anabolic insulin signaling in oxidative skeletal muscle.

MATERIALS AND METHODS

Animal Treatments

All procedures were reviewed and approved by the Iowa State University Institutional Animal Care and Use Committee (Protocol #2-12-7307-S). Detailed descriptions of animal treatments and previous data have been previously published (Cruzen et al., 2015; Pearce et al., 2015a, 2015b; Ganesan et al., 2016, 2017). Briefly, 24 individually penned crossbred gilts (64 ± 3 kg BW, mean ± SE) were allocated to one of three environmental treatments: (1) thermal neutral ad libitum (**TN**; 21 °C, 40% humidity, n = 8); (2) HS ad libitum (HS; 37 °C, 40% humidity, n = 8); or (3) pair-fed thermal neutral (**PFTN**; feed intake matched to HS counterparts and reared in TN conditions, n = 8/group). All pigs had ad libitum access to water and were fed throughout the study period as previously described (Pearce et al., 2015b). Following a 12 h environmental exposure, gilts were euthanized and the red portion of the semitendinosus (**STR**) was collected and stored in liquid nitrogen for later analyses.

Immunochemistry

Whole homogenate and nuclear fraction protein (NE-PER Nuclear and Cytoplasmic Extraction Kit, Thermo scientific, Rockford, IL) were isolated from 50 mg of muscle as previously described (Ganesan et al., 2016). Briefly, muscle was powered on dry ice, protein extracted, and concentration measured using a BCA kit (Pierce BCA microplate protein assay kit, Pierce, Rockford, IL). Membrane fraction protein was isolated using a Plasma Membrane Protein Extraction Kit according to manufacturer's protocol (Abcam, Cambridge, MA). Briefly, 20 mg of STR was powdered on dry ice and homogenized with 500 µl of 1X homogenizing buffer. The homogenate was centrifuged at 700 × g for 10 min at 4 °C. Collected supernatant was again centrifuged at 10,000 × g for 30 min at 4 °C. The resultant pellet contained proteins from the plasma membrane and the protein concentration was measured using a BCA kit.

Homogenates were diluted to 4 mg/ml in loading buffer (Bio Rad cat no. 1610737) and β-mercaptoethanol (Bio Rad cat no. 1610710). Forty micrograms of protein were loaded into each well in 4–20% precast gradient gel and proteins were electrophoresed at room temperature for 10 min at 60 V followed by 60 min at 120 V. Afterward, proteins were transferred (60 min; 100 V) to a nitrocellulose membrane (Bio Rad cat no. 1620112). Membranes were blocked for 1 h in 5% nonfat dry milk in Tris-buffered saline containing 0.2% Tween 20 (**TTBS**). Membranes with protein from whole homogenate were incubated with primary antibody overnight at 4 °C (Tables 1 and 2). Following three washes in TTBS, membranes were incubated with species-specific secondary antibodies (in dilutions as mentioned in Tables 1 and 2, anti-rabbit: cat. no 7074, anti-mouse: cat. no 7076, Cell Signaling Technology) for 1 h at room temperature. Membranes were washed three times in TTBS and incubated in enhanced chemiluminescence detection substrate (ECL Plus, GE Healthcare Bio-Sciences, Pittsburgh, PA) for 5 min and then membranes were exposed to X-ray film. Net intensity of each band was determined using Carestream 5.0 molecular imaging software (Carestream Health, New Haven, CT). The optical density was normalized to TN values. To confirm equal loading, all membranes were stained with Ponceau S and the resultant images captured and lane optical densities quantified. In all instances, resultant Ponceau S signal was similar between groups.

Table 1. Antibodies and dilutions used in immunoblotting to determine expression of proteins involved in insulin, PI3K, AKT, and PKC signaling and glucose transport

Antibody	Primary dilution	Secondary dilution	Company	Product no
Insulin receptor beta (IRβ)	1:1000	1:3000	Cell Signaling Technology	3025
Phospho-insulin receptor substrate 1 (pIRS-1 ^{Ser307})	1:1000	1:3000	Cell Signaling Technology	2381
Phospho-IRS-1 (pIRS-1^{Ser612})	1:1000	1:3000	Cell Signaling Technology	3203
Phosphatidylinositide 3-kinase (PI3Kp110)	1:1000	1:3000	Cell Signaling Technology	4255
Phospho-phosphoinositide-dependent kinase-1 (pPDPK1 ^{Ser241})	1:1000	1:3000	Cell Signaling Technology	3438
Protein kinase B (AKT)	1:1000	1:3000	Cell Signaling Technology	9272
Phospho-AKT ^{Thr308}	1:1000	1:3000	Cell Signaling Technology	9275
Phospho-AKT^{S473}	1:1000	1:3000	Cell Signaling Technology	9271
Protein phosphatase 2A (PP2AC)	1:1000	1:2000	Cell Signaling Technology	2038
Phospho-Protein Kinase C (pPKCδ/θ $^{Ser643/676}$)	1:1000	1:3000	Cell Signaling Technology	9376
Phospho-PKCζ/λ$^{Thr410/403}$	1:1000	1:3000	Cell Signaling Technology	9378
Phospho-AKT substrate of 160 kDa (pAS160^{Ser588})	1:1000	1:3000	Cell Signaling Technology	8270
Ras-related protein (Rab5)	1:1000	1:2000	Cell Signaling Technology	2143
Vesicle-associated membrane protein 2 (VAMP2)	1:1000	1:2000	Abcam	ab3347
Glyceraldehyde 3-phosphate dehydrogenase (GAPDH)	1:1000	1:2000	Santa Cruz Biotechnology	SC-47724
NA^+, K^+ -ATP ase	1:1000	1:2000	Cell Signaling Technology	3010
Glucose transporter type 4 (GLUT4)	1:1000	1:4000	Abcam	ab654

Table 2. Antibodies and dilutions used in immunoblotting to determine expression of proteins involved in protein, fatty acid, and glycogen metabolism

Antibody	Primary dilution	Secondary dilution	Company	Product no.
Mechanistic Target of Rapamycin (mTOR)	1:1000	1:3000	Cell Signaling Technology	2983
Phospho-mTOR (pmTOR ^{Ser2448})	1:750	1:3000	Cell Signaling Technology	2971
Phospho-P70S6 Kinase (pP70S6K ^{Thr389})	1:1000	1:3000	Cell Signaling Technology	9234
4E-binding protein 1 (4EBP1)	1:750	1:3000	Cell Signaling Technology	9644
Phospho-4EBP1 (p4EBP1$^{Thr37/46}$)	1:1000	1:3000	Cell Signaling Technology	2855
Acetyl-CoA carboxylase (ACC)	1:1000	1:3000	Cell Signaling Technology	3676
Phospho-ACC (pACC ^{S79})	1:1000	1:3000	Cell Signaling Technology	11818
ATP citrate lyase (ATPCL)	1:1000	1:3000	Cell Signaling Technology	4332
Phospho-ATP citrate lyase (ATPCL ^{Ser455})	1:1000	1:3000	Cell Signaling Technology	4331
Fatty acid synthase (FAS)	1:1000	1:3000	Cell Signaling Technology	3180
Glycogen synthase kinase 3 beta (GSK3β)	1:1000	1:3000	Cell Signaling Technology	9315
Phospho-GSK3β (pGSK3β ^{Ser9})	1:1000	1:3000	Cell Signaling Technology	9323
Phospho-GSK3β (pGSK3β ^{Thy216})	1:1000	1:3000	Santa Cruz Biotechnology	SC-35653
Glycogen synthase (GS)	1:1000	1:3000	Cell Signaling Technology	3893
Phospho-GS (pGS^{Ser641})	1:1000	1:3000	Cell Signaling Technology	3891

GC-MS Analysis

Ribitol (25 µl from 1 mg/ml stock) was added to 20–40 mg of powdered sample as an internal standard for polar compounds. Alternatively, 20 µl nonadecanoic acid (**NAA**; from 1 mg/ml stock) was added to samples as an internal standard for nonpolar compounds. Then, 0.35 ml of hot methanol (60 °C) was added to the samples and incubated at 60 °C for 10 min. Samples were vortexed for 10 s and placed into a sonication water bath for 10 min at full output power. Next, 0.35 ml of chloroform was added to the samples and vortexed for 30 s followed by 0.3 ml of water and another 30 s vortexing bout. The samples were centrifuged for 5 min at maximum speed. Two hundred microliters of upper layer (polar fraction) and 200 µl of lower layer (nonpolar fraction) were added into GC-MS vials. Samples were dried in a speed-vac concentrator for 6 to 10 h and then 50 µl of (20 mg/ml of pyridine) methoxyamine hydrochloride was added to dried polar extract followed by a 1.5 h incubation 30 °C with continuous shaking. Trimethylsilylation (**TMS**) was performed by addition of 70 µl of bis-trimethyl silyl trifluoroacetamide with 1% Trimethylchlorosilane (BSTFA + 1% TMCS) for 30 min at 37 °C. TMS was performed on both nonpolar and polar

fractions. One microliter of sample was injected for GC-MS analysis.

GC-MS analyses were performed with an Agilent 6890N gas chromatograph coupled to a model 5975 Mass Selective Detector (Agilent Technologies, Palo Alto, CA). The column used was HP-5MS 5% Phenyl Methyl Silox with 30 m × 250μM × 0.25 μm film thickness (Agilent Technologies). For nontargeted metabolite analysis, oven temperature was programmed as follows: 80 °C for 1 min, increase to 200 °C at a rate of 10 °C/min and hold for 5 min, and then increase to 320 °C at 10 °C/min and hold for 5 min. Helium was used as a carrier gas at a flow rate of 2 ml/min. Quantification was performed using electron ionization at 70 eV and source temperature and quadrupole temperature were set at 230 °C and 150 °C, respectively. The mass data were collected in the range from m/z 40 to m/z 1,000. The identification of compounds was facilitated by using Agilent Enhanced ChemStation version D.02.00.275 and the quantification was calculated by integrating the corresponding peak areas relative to the area of the internal standard.

Raw data were normalized to the amount of tissue used. Metabolomics data and pathway enrichment analysis were conducted using MetaboAnalyst (version 3.0), Pathway Analysis module (Xia et al., 2015). The module uses curated KEGG metabolic pathways as the backend knowledgebase. In the first step, the compound names were matched against the other databases to standardize compound labels. The standardized labels were then searched against Human pathway library (Kanehisa et al., 2017). The quantitative enrichment analysis was performed using the compound concentration values to detect changes among the compounds involved in the same biological pathway. The Tables (3 and 4) show the detailed results from the pathway analysis. Since we tested multiple pathways simultaneously, the statistical *P* values from enrichment analysis are further adjusted for multiple testings. For purposes of clarity and to provide readers additional information all significant pathways identified in our analysis are included. The Holm *P* is the *P* value adjusted by Holm–Bonferroni method.

Statistics

To determine the effect of HS, data from TN, HS, and PFTN animals were compared using one-way ANOVA followed by Newman–Keuls post hoc test (GraphPad prism, version 5). Statistical significance was set at $P < 0.05$. Values are reported as mean ± SE.

RESULTS

Heat Load Caused a Physiological HS Response

A detailed HS response to an environmental heat load has been previously published (Cruzen et al., 2015; Pearce et al., 2015a, 2015b; Ganesan et al., 2016, 2017). Following 12 h of HS, the rectal temperatures in TN (39.2 ± 0.12 °C) and pair-fed TN (39.1 ± 0.12 °C) groups were similar, whereas heat-stressed pigs were increased compared to both groups (41.5 ± 0.13 °C; $P < 0.05$; Pearce et al., 2015a). Animals maintained under TN conditions consumed approximately 1 kg feed during the 12 h treatment period and the heating intervention (and pair feeding) resulted in an approximate 90% reduction in feed intake (Pearce et al., 2015a). Correspondingly, TN animals gained 0.39 kg during this period, whereas pair-fed animals lost 1.87 kg and hyperthermic animals lost 4.56 kg (all groups different from each other; Pearce et al., 2015a). Circulating insulin was decreased in heat-stressed animals (0.04 ng/dl) compared to TN (0.18 ng/dl) and PFTN (0.10 ng/dl) animals (Pearce et al., 2015b). However, circulating glucose concentration was similar between groups (TN: 99.2 mg/dl; HS: 98.0 mg/dl; and PFTN: 94.4 mg/dl). Plasma NEFA was increased in heat-stressed animals (0.25 nmol/l) compared to TN (0.09 nmol/l) and PFTN (0.12 nmol/l) animals (Pearce et al., 2015b).

Heat Load Altered Upstream Insulin Signaling

HS increased ($P = 0.005$) the relative protein abundance of insulin receptor (**IRβ**) by 0.54 ± 0.16 fold compared to TN and 0.59 ± 0.11 fold compared to PFTN (Figure 1A and B). Phosphorylation of IR substrate 1 (IRS1) at several serine sites blunts insulin signaling. Despite increased insulin receptor abundance in heat-stressed muscle, $pIRS1^{S307}$ protein abundance was increased ($P = 0.0005$) by HS compared to TN (0.56 ± 0.09 fold) and PFTN (0.51 ± 0.09 fold). Protein abundance of $pIRS1^{S612}$ was also increased numerically ($P = 0.07$) in HS compared to TN (0.70 ± 0.30 fold) but did not reach statistical significance. IRS1 client protein phosphatidylinositide 3-kinases (PI3 kinase) was similar between groups ($P = 0.50$); however, phosphorylation of phosphoinositol-dependent kinase 1 at serine 241 ($PDPK1^{S241}$), downstream of PI3 kinase, was increased ($P = 0.02$) in HS compared to TN (0.39 ± 0.17 fold) and PFTN (0.5 ± 0.1 fold)

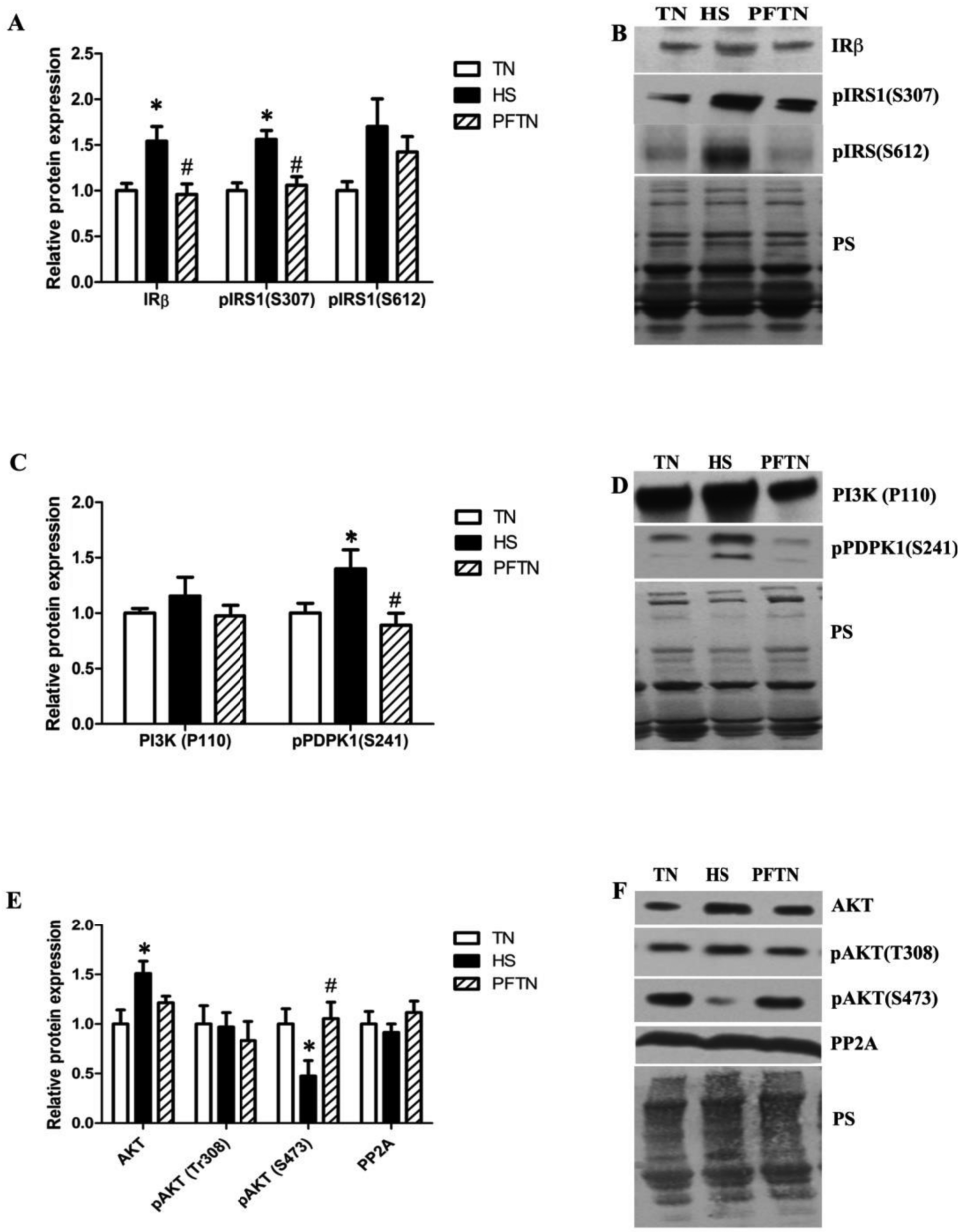

Figure 1. Heat load altered upstream insulin signaling. Following 12 h of HS, Insulin signaling: insulin receptor beta (IRβ), Phosphorylated insulin receptor substrate 1 (pIRS1^{Ser307}), and Phosphorylated IRS1 (pIRS1^{Ser612}) (A, B), PI3K signaling: Phosphatidylinositide 3-kinase (PI3Kp110) and phosphorylated phosphoinositide-dependent kinase-1 (pPDPK1^{Ser241}) (C,D) and AKT signaling: Protein kinase B (AKT), Phosphorylated AKT^{Thr308}, Phosphorylated AKT^{S473} and Protein phosphatase 2A (PP2AC) (E, F) protein expressions were measured by Western blot in the TN, HS and PFTN groups. Representative blots are included. Ponceau S stain (PS) was used as a loading control. Values are mean ± SE; n = 8/group. * indicates significantly different from TN ($P < 0.05$); #indicates significantly different from HS ($P < 0.05$).

(Figure 1C and D), suggesting increased PI3 kinase activity.

Full activation of protein kinase B (**AKT**) is dependent on phosphorylation of serine 473 (S473) by mechanistic target of rapamycin complex 2 (**mTORC2**) and threonine 308 (**T308**) by PDPK1. HS caused a 0.50 ± 0.12 fold increase (P = 0.02) in AKT protein abundance compared to TN while PFTN was similar to both groups (Figure 1E and F). Though phosphorylated AKT^{T308} was similar (P = 0.70) between groups, phosphorylated AKT^{S473} was decreased 0.53 ± 0.15 and 0.58 ± 0.16 fold in HS compared to TN and PFTN (P = 0.03), respectively, indicating suppressed AKT signaling. Since upstream signaling did not account for the reduction in pAKT^{S473} by HS, we also measured the relative abundance of a known AKT phosphatase, protein phosphatase 2A (**PP2A**). However, PP2A content was similar between (P = 0.44) groups (Figure 1E and F).

Heat Load Altered Protein Kinase C Signaling

In addition to AKT, the atypical protein kinase C (**PKC**) isoforms zeta and lambda (**PKCζ/λ**) are

phosphorylated and activated by PDPK1. These isoforms are involved with glucose transporter type 4 (**Glut4**) translocation and glucose uptake, and may also regulate insulin signaling (Tobias et al., 2016). Protein abundance of phosphorylated PKCζ/λ$^{Thr410/403}$ was increased (P = 0.02) in HS (0.28 ± 0.09 fold) and PFTN (0.27 ± 0.05 fold) compared to TN (Figure 2A and B). Similarly, PKCζ/λ$^{Thr410/403}$ protein abundance in the membrane fraction was increased (P = 0.01) by HS (0.82 ± 0.16 fold) compared to TN (Figure 2C and D), supporting its activation and potential role in stimulating glucose uptake independent of insulin signaling (Tremblay et al., 2001). PKCδ/θ, novel isoforms of protein kinase C, phosphorylate a multitude of inhibitory serine sites on IRS1, leading to inhibition of insulin signaling (Schmitz-Peiffer and Biden, 2008). Protein abundance of phosphorylated PKCδ/θ$^{S643/676}$ was increased (P = 0.02) by 1.05 ± 0.35 fold in HS compared to TN while PFTN was similar to both groups (Figure 2A and B).

Heat Load Reduced Sarcolemma Glucose Transporter

AKT plays a role in insulin-mediated regulation of glucose transport via phosphorylation of AKT substrate of 160 kDa (AS160). The relative abundance of Glut4 in the sarcolemma fraction was (P = 0.04) decreased 0.47 ± 0.06 fold in HS compared to TN, whereas PFTN did not differ from other groups (Figure 3A and B). However, relative abundance of Glut4 in the cytoplasmic fraction was (P = 0.55) similar between groups (Figure 3C and D). Markers of cytoplasmic fraction (GAPDH) and membrane fraction (NA+, K+-ATPase) were used to verify the purity of each fraction (Figure 3E). In addition, phosphorylated AS160^{S588} was similar between (P = 0.21) groups. RAB5 (P = 0.41) and vesicle-associated membrane proteins (**VAMP**) 2 (P = 0.44) are essential for movement and docking of Glut4 storage vesicles with the plasma membrane and were also similar between groups (Figure 3F and G).

Heat Load Altered Protein Synthesis Machinery

Anabolic effects of insulin are attributed to the phosphorylation and activation of mechanistic target of rapamycin (**mTOR**). HS increased total mTOR protein abundance (P = 0.04) by 1.40 ± 0.47 fold compared to TN, and PFTN was similar to HS and TN; phosphorylated mTOR^{Ser2448} protein abundance (P = 0.08) was similar between groups. Protein abundance of eukaryotic translation initiation factor 4E-binding protein 1 (**4EBP1**), a translational repressor, was (P = 0.04) increased 1.23 ± 0.44 fold in HS compared to TN, and PFTN was similar to HS and TN. Importantly, phosphorylation of 4EBP1 (p4EBP1$^{Thr37/46}$), an inactive

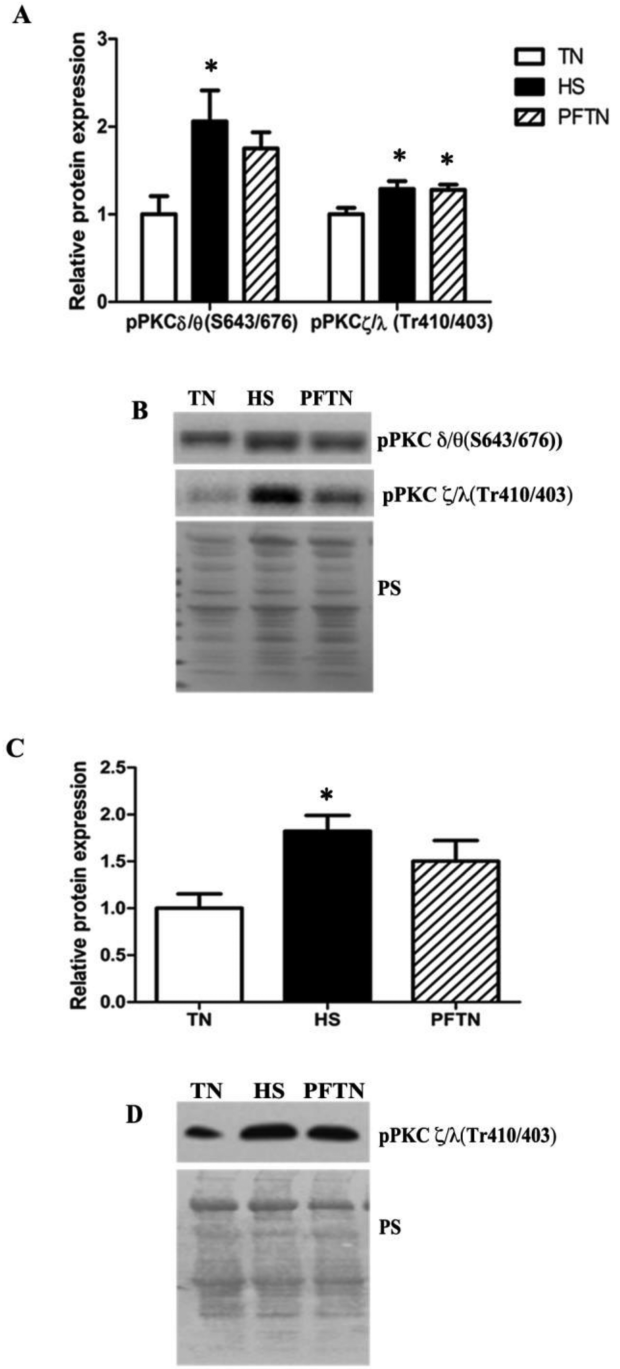

Figure 2. Heat load altered protein kinase C signaling. Following 12 h of HS, PKC signaling: Phosphorylated Protein Kinase C (pPKCδ/θ $^{Ser643/676}$), Phosphorylated PKCζ/λ$^{Thr410/403}$ protein expressions were measured by Western blot in the TN, HS and PFTN groups in whole homogenate and (A, B) in membrane fraction (C, D). Representative blots are included. Ponceau S stain (PS) was used as a loading control. Values are mean ± SE; n = 8/group. *Indicates significantly different from TN (P < 0.05); #indicates significantly different from HS (P < 0.05).

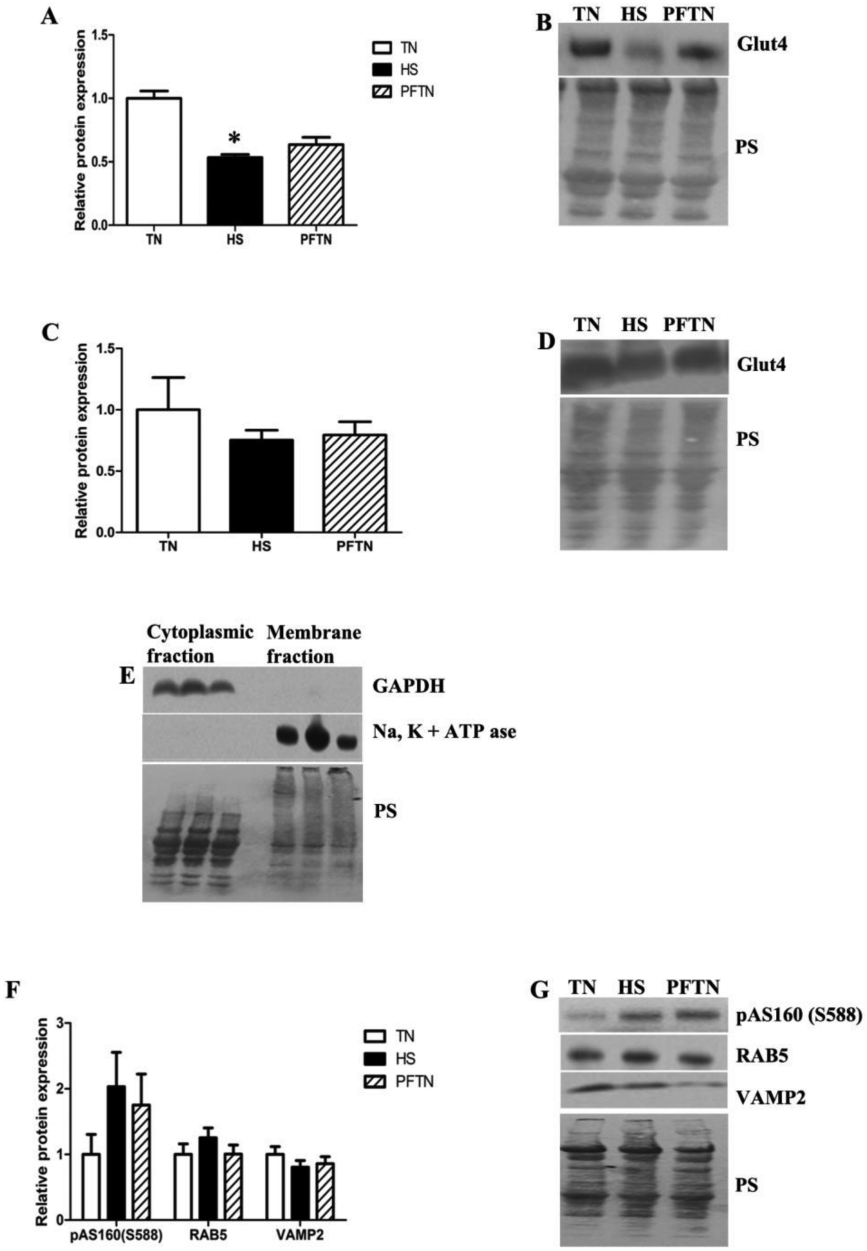

Figure 3. Heat load reduced sarcolemma glucose transporter. Following 12h of HS, Glucose transporter type 4 (GLUT4) (A–D), NA^+, K^+ -ATP ase, Glyceraldehyde 3-phosphate dehydrogenase (GAPDH) (E) from membrane and cytoplasmic fraction and Phospho-AKT substrate of 160 kDa ($pAS160^{Ser588}$), Ras-related protein (Rab5), Vesicle-Associated Membrane Protein 2 (VAMP2) protein expressions in whole homogenate (F, G) and were measured by Western blot in the TN, HS and PFTN groups. Representative blots are included. Ponceau S stain (PS) was used as a loading control. Values are mean ± SE; n = 8/group. *Indicates significantly different from TN ($P < 0.05$); #indicates significantly different from HS ($P < 0.05$).

form ($P = 0.19$), was similar between groups as was phosphorylated ribosomal protein S6 kinase beta-1 ($p70S6K^{Thr389}$; $P = 0.21$; Figure 4A and B).

Heat Load and Feed Intake Altered Glycogen Metabolism Markers

AKT also plays a role in glycogen metabolism by regulating glycogen synthase (**GS**) kinase 3 (**GSK3β**). Following 12 h of HS protein abundance of total GSK3β, $pGSK3\beta^{S9}$, and $pGSK3\beta^{Tyr216}$ was similar between groups. However, GS protein abundance was decreased ($P = 0.0006$) 0.32 ± 0.05 fold in HS and by 0.19 ± 0.06 fold in PFTN compared to TN controls. In addition, phosphorylated GS^{Ser641} protein abundance, which inhibits GS activity, was ($P = 0.02$) increased 0.34 ± 0.12 fold in HS and 0.43 ± 0.10 fold in PFTN compared to TN pigs (Figure 5A and B).

Heat Load Altered Fatty Acid Metabolism Markers

We have previously established that HS caused an increase ($P = 0.01$) in phosphorylated

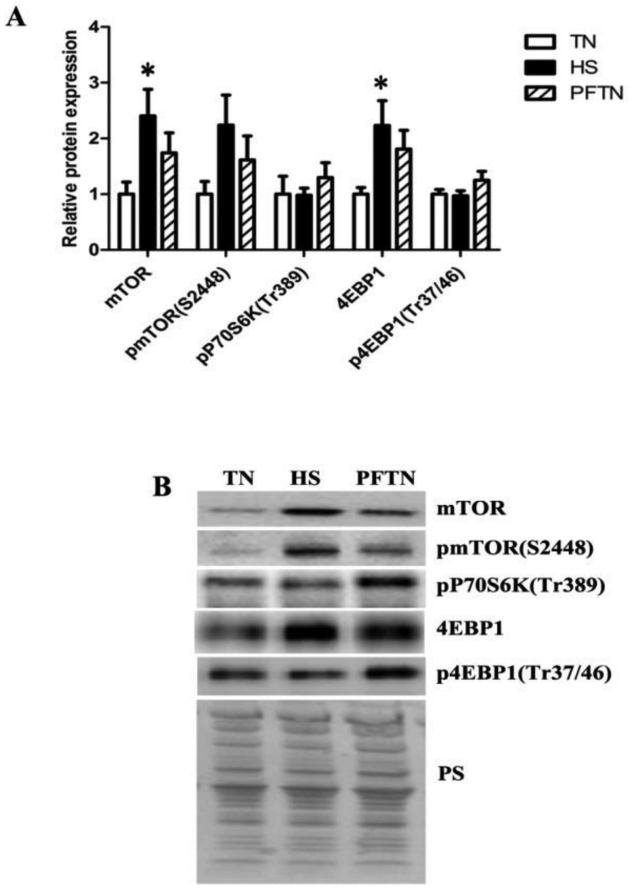

Figure 4. Heat load altered protein synthesis machinery. Following 12 h of HS, Mechanistic Target of Rapamycin (mTOR), Phosphorylated mTOR ($pmTOR^{Ser2448}$), Phosphorylated P70S6 Kinase ($pP70S6K^{Thr389}$), 4E-binding protein 1 (4EBP1) and Phosphorylated 4EBP1 ($p4EBP1^{Thr37/46}$) protein expressions in whole homogenate were measured by Western blot in the TN, HS, and PFTN groups (A, B). Representative blots are included. Ponceau S stain (PS) was used as a loading control. Values are mean ± SE; n = 8/group. *Indicates significantly different from TN ($P < 0.05$); #indicates significantly different from HS ($P < 0.05$).

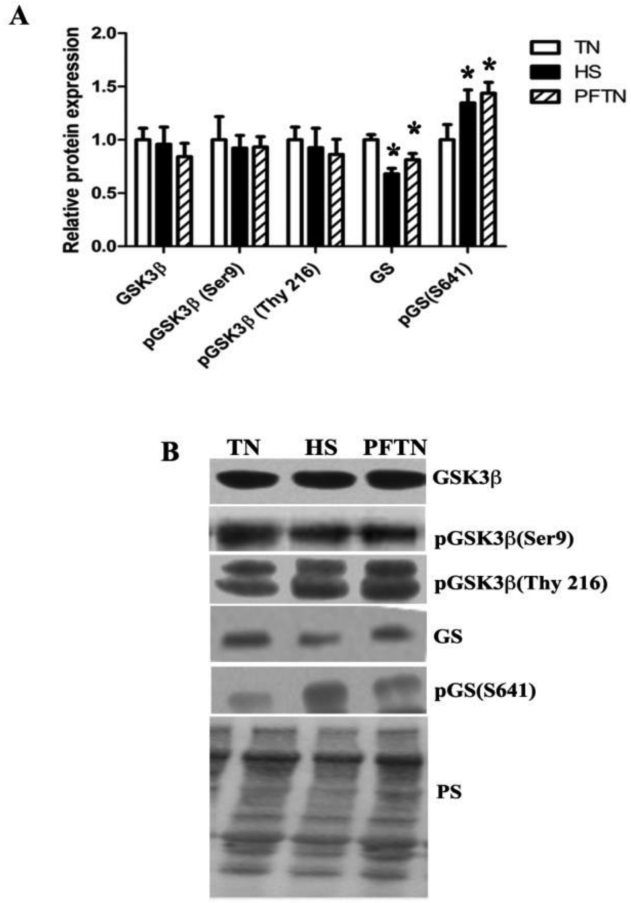

Figure 5. Heat load altered glycogen metabolism signaling. Following 12 h of HS Glycogen synthase kinase 3 beta (GSK3β), Phosphorylated GSK3β ($pGSK3\beta^{Ser9}$), Phosphorylated GSK3β ($pGSK3\beta^{Thy216}$), Glycogen synthase (GS), and Phosphorylated GS (pGS^{Ser641}) protein expressions in whole homogenate were measured by Western blot in the TN, HS, and PFTN groups (A, B). Representative blots are included. Ponceau S stain (PS) was used as a loading control. Values are mean ± SE; n = 8/group. *Indicates significantly different from TN ($P < 0.05$); #indicates significantly different from HS ($P < 0.05$).

AMP-activated protein kinase (**AMPK**) (1.7 ± 0.58 fold) in tissues used in this investigation (Ganesan et al., 2017). We now report a 0.68 ± 0.21 and 0.74 ± 0.15 fold increase (P = 0.02) in Acetyl-CoA carboxylase (**ACC**) protein abundance in HS and PFTN compared to TN, respectively; however, $pACC^{S79}$ was similar between groups (P = 0.16). In addition, while total ATP-citrate lyase (**ATPCL**) was similar between groups, phosphorylated $ATPCL^{S455}$ was decreased (P = 0.005) by 0.59 ± 0.08 fold in HS compared to TN and fatty acid synthase (**FAS**) was decreased (P = 0.01) by 0.37 ± 0.13 and 0.44 ± 0.11 fold in HS compared to TN and PFTN, respectively (Figure 6A and B).

Metabolomics Pathway Analysis

Our hypothesis-driven assessment of pathways representing protein metabolism, glycogen metabolism, fatty acid metabolism, and glucose transport indicate physiological impacts of both HS and caloric restriction. To provide additional confirmation of these findings, we performed a metabolomics experiment that further implicated alterations in protein synthesis in the HS response as changes in metabolic pathways including alanine, aspartate, glutamate, arginine, proline, glycine, serine, threonine, tyrosine, cysteine, methionine, tryptophan, and phenylalanine metabolism were significantly ($P < 0.05$) altered by the treatments (Tables 3 and 4). In addition, we also found that carbohydrate metabolism was implicated as the citric acid cycle, pentose phosphate pathway, and carbohydrate metabolism were identified (Tables 3 and 4). Lastly, and consistent with our previous biochemical findings, fatty acid synthesis was implicated ($P < 0.05$; Table 4).

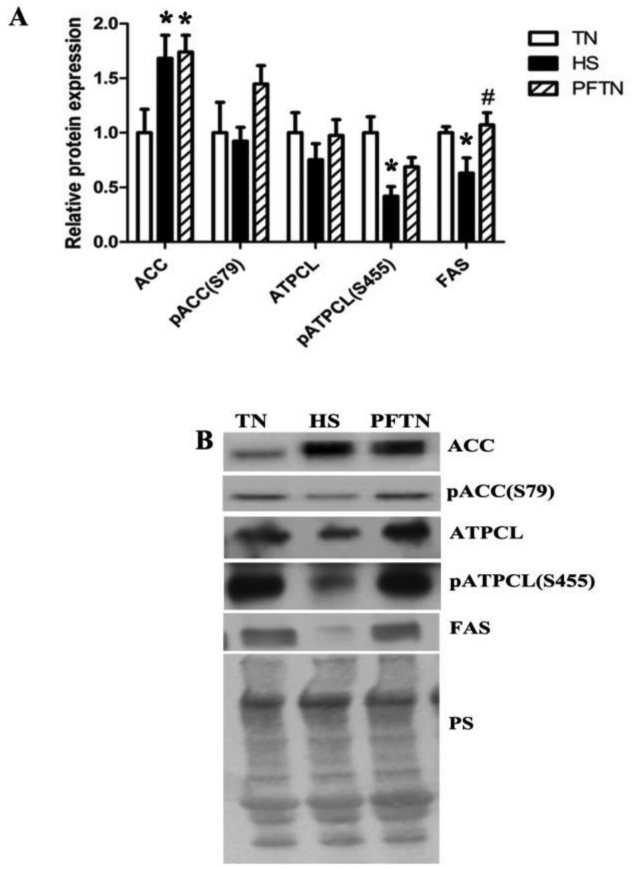

Figure 6. Heat load altered fatty acid metabolism signaling. Following 12 h of HS, Acetyl-CoA carboxylase (ACC), Phosphorylated ACC (pACC^{S79}), ATP-citrate lyase (ATPCL) and Phosphorylated ATP-citrate lyase (ATPCL^{Ser455}) protein expressions in whole homogenate were measured by Western blot in the TN, HS, and PFTN groups (A, B). Representative blots are included. Ponceau S stain (PS) was used as a loading control. Values are mean ± SE; n = 8/group. *Indicates significantly different from TN ($P < 0.05$); #indicates significantly different from HS ($P < 0.05$).

Table 3. Pathway analysis for polar metabolites

KEGG pathways	Raw *P* value	Holm adjust *P* value
Aminoacyl-tRNA biosynthesis	1.04E−09	8.28E−08
Alanine, aspartate and glutamate metabolism	4.35E−08	3.44E−06
Nitrogen metabolism	2.05E−07	1.60E−05
Citrate cycle (TCA cycle)	8.72E−05	0.0067149
Arginine and proline metabolism	0.00045068	0.034252
Cyanoamino acid metabolism	0.00047591	0.035693
Glycine, serine and threonine metabolism	0.00092448	0.068412
Galactose metabolism	0.0028401	0.20732
Glyoxylate and dicarboxylate metabolism	0.0067845	0.48849
Starch and sucrose metabolism	0.0067845	0.48849
Pentose phosphate pathway	0.0070155	0.49108
Phenylalanine metabolism	0.022955	1.0000
Phenylalanine, tyrosine and tryptophan biosynthesis	0.026953	1.0000
D-Glutamine and D-glutamate metabolism	0.028187	1.0000
Tyrosine metabolism	0.036471	1.0000
Cysteine and methionine metabolism	0.046411	1.0000

Table 4. Pathway analysis for nonpolar metabolites

KEGG pathways	Raw *P* value	Holm adjust *P* value
Fatty acid biosynthesis	0.00013548	0.010838
Galactose metabolism	0.009089	0.71803
Citrate cycle (TCA cycle)	0.018921	1.0000
Arginine and proline metabolism	0.048258	1.0000

DISCUSSION

HS antagonizes lean disuse deposition and protein synthesis in meat animal production. A better understanding of the molecular mechanisms underlying HS-mediated dysfunction in muscle is critical to develop effective treatment protocols and mitigation strategies. Changes in systemic and intracellular energy metabolism, specifically skeletal muscle metabolic signaling, are critical for adaptation and survival during increased heat load. Previously, we reported that the animals used in this study exhibited decreased circulating insulin and increased NEFA and plasma urea nitrogen without alterations in blood glucose compared to a TN controls (Pearce et al., 2015b). We also reported reduced circulating inflammatory markers (Pearce et al., 2015b) concomitant with evidence of skeletal muscle inflammatory signaling (Ganesan et al., 2016), oxidative stress (Cruzen et al., 2015; Ganesan et al., 2017), and mitochondrial dysfunction (Ganesan et al., 2017). Given these systemic and skeletal muscle-specific changes, we hypothesized that HS would alter intracellular insulin signaling in oxidative skeletal muscle. We found that HS-altered markers of glucose transport and protein, glycogen, and fatty acid metabolism (Figure 7) through impaired insulin signaling.

Insulin is a major anabolic hormone controlling critical energy functions including glucose and lipid metabolism. Insulin stimulates glucose uptake through an intracellular signaling cascade that leads to membrane translocation of Glut4. Our data indicate that sarcolemma Glut4 transporter protein abundance was impaired by HS, which is consistent with reduced circulating insulin and feed intake. Notably, this result is in contrast to a therapeutic hyperthermia intervention in which a brief exposure to heat maintained insulin sensitivity and Glut4 protein abundance in skeletal muscle in a diabetes model (Goto et al., 2015). HS-induced

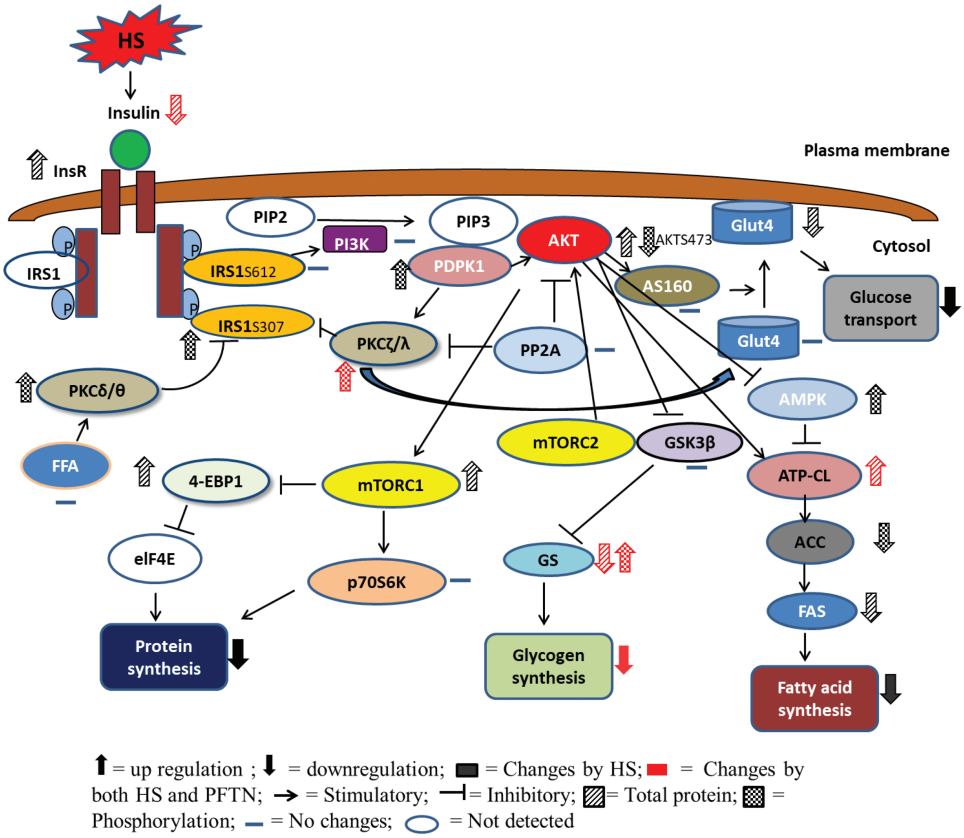

Figure 7. Heat load impaired intracellular signaling in skeletal muscle. Heat stress altered protein metabolism, glycogen metabolism, and fatty acid metabolism through impaired protein kinase B (AKT) signaling. Functional outcomes denoted here are hypothetical and are based on observed changes in signaling cascades.

signaling changes implicated by impaired Glut4 translocation were investigated in more detail.

Insulin activates the insulin receptor tyrosine kinase, which phosphorylates and recruits different substrate adaptors, such as the IRS family of proteins. Following 12 h of HS it seems muscle cells are attempting to maintain insulin signaling by increasing insulin receptor abundance in the face of decreasing blood insulin but are simultaneously and paradoxically inhibiting insulin receptor substrate via increased phosphorylation of IRS1^{S307} (Gao et al., 2015b). The activity of PI3K by its catalytic p110 subunit is required for the generation of PIP3, which in turn recruits and phosphorylates PDPK^{S241} to completely activate AKT (Madhunapantula and Robertson, 2011; Davies, 2012). Though P13K (p110) was similar between groups, phosphorylated AKT^{Thr308} may have been maintained by increased pPDPK1^{S241}. In addition, PP2A was similar between groups, suggesting that HS was not inhibiting AKT through dephosphorylation at Thr308 (Kuo et al., 2008). Phosphorylation of AKT^{S473} by mTOR is also required for its full activation (Vivanco and Sawyers, 2002; Xu et al., 2012). Phosphorylated AKT^{S473} was decreased by HS, which was in good agreement with previous work demonstrating an interaction of temperature and pAKT^{S473} (Oehler-Jänne et al., 2008).

Despite elevated pPDPK1^{S241} and translocation of pPKCζ/λ$^{Thr410/403}$ to the sarcolemma, sarcolemmal Glut4 abundance was decreased following HS indicating PKCζ/λ$^{Thr410/403}$ did not play a role in presumptive HS-induced reductions in glucose uptake in skeletal muscle. Although activation of atypical PKC isoforms λ and ζ is necessary for insulin-mediated stimulation of glucose uptake (Standaert et al., 1997; Kotani et al., 1998; Bandyopadhyay et al., 2000) this alone is insufficient, and may actually provide negative feedback on the insulin signaling pathway through pIRS-1^{S318} and inhibition of AKT^{T308}, as observed here (Ravichandran et al., 2000; Moeschel et al., 2004; Tobias et al., 2016). Though PDPK1 directly activates atypical PKC isoforms (Le Good et al., 1998), PKCζ/λ protein expression can be stimulated, at least in part, by tumor necrosis factor (TNFα), independent of insulin (Tremblay et al., 2001). Indeed, we have previously shown increased intramuscular TNFα abundance following 12 h and 24 h of HS (Montilla et al., 2014; Ganesan et al., 2016), suggesting that increased PKCζ/λ protein abundance might be due to the proinflammatory effect of HS.

Similarly, phosphorylation of novel PKCδ/θ$^{S643/676}$ was increased by HS possibly through increased FFA (Spitzer and Deaciuc, 1992) as we have previously reported in these animals. Additionally, elevated FFA (and ceramides) can inhibit AKT activity through increased atypical PKC activity independent of PDPK1 signaling (Hage Hassan et al., 2014). The novel PKC isoforms have been shown to inhibit insulin signaling in skeletal muscle through inhibition of IRS1 (Kim et al., 2004). These data indicate that PKC isoforms play a major role in regulation insulin signaling during HS.

Insulin stimulates protein synthesis by activating protein kinases AKT and mTOR (Wang and Proud, 2006; Haar et al., 2007) and leads to subsequent phosphorylation of 4EBP1 and activation of eIF4E (Gingras et al., 1999), thus promoting translation. In this study, HS increased total mTOR and 4EBP1 but not pmTOR, p-p70S6K, or p4EBP1, raising the possibility that HS blunts initiation of protein translation in muscle (Hickey and Weber, 1982; Duncan and Hershey, 1989; Kregel, 2002). Indeed, such a HS-mediated suppression of protein synthesis may be supported by excessive loss of body mass compared to pair-fed animals and increased plasma urea nitrogen compared to TN and pair-fed animals. Moreover, numerous KEGG pathways involving amino acids and protein synthesis were identified in our metabolomics experiments. A similar failure to increase p4EBP1 protein abundance was found in satellite cells following HS (Gao et al., 2015a). These biochemical findings are supported by the phenotypic increase in skeletal muscle catabolism during HS in variety of species (Marder et al., 1990; Geraert et al., 1996; Yunianto et al., 1997; Wheelock et al., 2010; Johnson et al., 2015) and increased adiposity at the expense of muscle mass HS pigs (Heath, 1983; Johnson et al., 2015).

In the absence of insulin, GSK3 maintains the phosphorylation state of the multiple serine residues on IRS1, thereby limiting insulin receptor signaling (Eldar-Finkelman, 2002). In addition, GSK3 phosphorylates GS to inhibit glycogen synthesis (Eldar-Finkelman et al., 1996). Though HS did not alter GSK3 phosphorylation, GS protein abundance was decreased in HS and PFTN compared to TN concomitant with increased phosphorylation. These findings suggest that decreased nutrient intake, and not HS, per se, is responsible for alterations in glycogen metabolism. These data are consistent with previous work in which HS decreased glycogen content in rat skeletal muscle (Goto et al., 2015).

We also determined the extent to which HS altered fatty acid metabolism in oxidative skeletal muscle. Although the quantitative importance of fatty acid synthesis in skeletal muscle to whole-body energetics is negligible, such metabolic changes may play a role in marbling and may provide clues that explain why heat-stressed animals accumulate more fat than their feed intake predicts (Heath, 1983). With that caveat, these data suggest impaired fatty acid synthesis in HS muscle; however, muscle from PFTN animals appeared largely resistant to changes in fatty acid synthesis. Changes in fatty acid synthesis are supported by our more sensitive metabolomics approach, which specifically identified the fatty acid biosynthesis KEGG pathway. Perhaps, more energetically significant than fatty acid synthesis is fatty acid combustion by skeletal muscle mitochondria. Importantly, we and others have previously reported metabolic inflexibility (a reduced capacity to oxidize fatty acids) and mitochondrial dysregulation, which may have broad metabolic and physiological impacts. In addition to triggering oxidative stress and apoptotic signaling, mitochondrial dysregulation may also impair efficient carbohydrate utilization. This latter point is supported by our metabolomics analyses, which identified multiple KEGG pathways, in both polar and nonpolar fractions, related to carbohydrate metabolism and the TCA cycle.

It is important to recognize that during environmental hyperthermia pigs necessarily experience multiple stressors including decreased feed intake, oxidative stress, increased heat load, and endotoxemia, among others. Hence, the response to hyperthermia is also a response to multiple physiological insults. In this investigation, we controlled for reduced feed intake that accompanies hyperthermic exposure. By employing this approach we were able to identify the contribution of reduced feed intake during 12 h of environmental hyperthermia to the overall stress response. For example, decreased Glut4 translocation to the sarcolemma appears to be related to the reduced feed intake component of environmental hyperthermia, and indeed, is consistent with decreased circulating insulin found in both the HS and PFTN groups. Following 12 h of environmental hyperthermia decreased feed intake also appears to contribute in part to alterations in PKC signaling and protein, glycogen, and fatty acid metabolism. However, changes related to the insulin receptor were independent of reduced feed intake and are likely dependent on some other stressor caused by increased heat load.

In conclusion, 12 h of HS decreased basal insulin signaling by increasing inhibitory pIRS1^{S307}, which is a negative regulator of insulin signaling. This resulted in decreased AKT signaling, and ultimately decreased Glut4 translocation to the sarcolemma compared to TN muscle, despite HS-mediated increases in atypical PKC phosphorylation. In addition, HS maintained activity of 4EBP1, an important translational repressor, and suppressed energetic metabolism via decreased phosphorylated ATP-citrate lyase (**pATPCL**) and FAS compared to muscle held under TN conditions. HS decreased glycogen synthesis by increasing phosphorylation of GS, which is likely explained by the reduced feed intake that accompanies HS. While these changes may limit free radical production resulting from incomplete reduction of oxygen they also limit growth efficiency in production animals and underscore the complexity of intracellular signaling changes in mammalian skeletal muscle caused by HS.

LITERATURE CITED

Addabbo, F., M. Montagnani, and M.S. Goligorsky. 2009. Mitochondria and reactive oxygen species. Hypertension 53(6):885–892. doi:10.1161/hypertensionaha.109.130054

Bandyopadhyay, G., Y. Kanoh, M.P. Sajan, M.L. Standaert, and R.V. Farese. 2000. Effects of adenoviral gene transfer of wild-type, constitutively active, and kinase-defective protein kinase C-λ on insulin-stimulated glucose transport in L6 myotubes. Endocrinology 141(11):4120–4127. doi:10.1210/endo.141.11.7766

Baumgard, L.H., and R.P. Rhoads. 2013. Effects of heat stress on postabsorptive metabolism and energetics. Annu. Rev. Anim. Biosci. 1(1):311–337. doi:10.1146/annurev-animal-031412-103644

Becker, B.A., C.D. Knight, F.C. Buonomo, G.W. Jesse, H.B. Hedrick, and C.A. Baile. 1992. Effect of a hot environment on performance, carcass characteristics, and blood hormones and metabolites of pigs treated with porcine somatotropin. J. Anim. Sci. 70(9). doi:1992.7092732x

Caspani, M.L., M. Savioli, S. Crotti, P. Bruzzone, and L. Gattinoni. 2004. Heat stress: characteristics, pathophysiology and avoidable mistakes. Minerva Anestesiol. 70(7–8):617–624.

Collin, A., J. van Milgen, S. Dubois, and J. Noblet. 2001. Effect of high temperature and feeding level on energy utilization in piglets. J. Anim. Sci. 79(7):1849–1857. doi:2001.7971849x

Cruzen, S.M., S.C. Pearce, L.H. Baumgard, N.K. Gabler, E. Huff-Lonergan, and S.M. Lonergan. 2015. Proteomic changes to the sarcoplasmic fraction of predominantly red or white muscle following acute heat stress. J. Proteomics 128:141–153. doi:10.1016/j.jprot.2015.07.032

Davies, M.A. 2012. The role of the PI3K-AKT pathway in melanoma. Cancer J 18(2):142–147. doi:10.1097/PPO.0b013e31824d448c

Duncan, R.F., and J.W. Hershey. 1989. Protein synthesis and protein phosphorylation during heat stress, recovery, and adaptation. J. Cell. Biol. 109(4):1467–1481. doi:10.1083/jcb.109.4.1467

Eldar-Finkelman, H. 2002. Glycogen synthase kinase 3: an emerging therapeutic target. Trends Mol Med 8(3):126–132. doi:10.1016/S1471-4914(01)02266-3

Eldar-Finkelman, H., G.M. Argast, O. Foord, E.H. Fischer, and E.G. Krebs. 1996. Expression and characterization of glycogen synthase kinase-3 mutants and their effect on glycogen synthase activity in intact cells. Proc. Natl. Acad. Sci. U.S. A. 93(19):10228–10233.

Ganesan, S., C. Reynolds, K. Hollinger, S.C. Pearce, N.K. Gabler, L.H. Baumgard, R.P. Rhoads, and J.T. Selsby. 2016. Twelve hours of heat stress induces inflammatory signaling in porcine skeletal muscle. Am. J. Physiol. Regul. Integr. Comp. Physiol. 310(11):R1288–1296. doi:10.1152/ajpregu.00494.2015

Ganesan, S., C.M. Summers, S.C. Pearce, N.K. Gabler, R.J. Valentine, L.H. Baumgard, R.P. Rhoads, and J.T. Selsby. 2017. Short-term heat stress causes altered intracellular signaling in oxidative skeletal muscle. J Anim Sci 95(6):2438–2451. doi:10.2527/jas.2016.1233

Gao, C.-Q., Y.-l. Zhao, H.-C. Li, W.-G. Sui, H.-C. Yan, and X.-Q. Wang. 2015a. Heat stress inhibits proliferation, promotes growth, and induces apoptosis in cultured Lantang swine skeletal muscle satellite cells. J Zhejiang Univ Sci B 16(6):549–559. doi:10.1631/jzus.B1400339

Gao, T.-T., Z.-l. Qin, H. Ren, P. Zhao, and Z.-T. Qi. 2015b. Inhibition of IRS-1 by hepatitis C virus infection leads to insulin resistance in a PTEN-dependent manner. Virol. J. 12:12. doi:10.1186/s12985-015-0241-4

Geraert, P.A., J.C.F. Padilha, and S. Guillaumin. 1996. Metabolic and endocrine changes induced by chronic heatexposure in broiler chickens: growth performance, body composition and energy retention. Br. J. Nutr. 75(02):195–204. doi:10.1017/BJN19960124

Gingras, A.-C., B. Raught, and N. Sonenberg. 1999. eIF4 initiation factors: effectors of mRNA recruitment to ribosomes and regulators of translation. Annu. Rev. Biochem. 68(1):913–963. doi:10.1146/annurev.biochem.68.1.913

Goto, A., T. Egawa, I. Sakon, R. Oshima, K. Ito, Y. Serizawa, K. Sekine, S. Tsuda, K. Goto, and T. Hayashi. 2015. Heat stress acutely activates insulin-independent glucose transport and 5′-AMP-activated protein kinase prior to an increase in HSP72 protein in rat skeletal muscle. Physiol. Rep. 3(11):e12601. doi:10.14814/phy2.12601

Haar, E.V., S.-I. Lee, S. Bandhakavi, T.J. Griffin, and D.-H. Kim. 2007. Insulin signalling to mTOR mediated by the Akt/PKB substrate PRAS40. Nat Cell Biol 9(3):316–323. doi:10.1038/ncb1547

Hage Hassan, R., O. Bourron, and E. Hajduch. 2014. Defect of insulin signal in peripheral tissues: important role of ceramide. World J. Diabetes 5(3):244–257. doi:10.4239/wjd.v5.i3.244

Heath, M.E. 1983. The effects of rearing-temperature on body composition in young pigs. Comp. Biochem. Physiol. A Physiol. 76(2):363–366. doi:10.1016/0300-9629(83)90338–9

Hickey, E.D., and L.A. Weber. 1982. Modulation of heat shock polypeptide synthesis in HeLa cells during hyperthermia and recovery. Biochemistry (Mosc). 21(7):1513–1521. doi:10.1021/bi00536a008

Johnson, J.S., M.V. Sanz Fernandez, J.F. Patience, J.W. Ross, N.K. Gabler, M.C. Lucy, T.J. Safranski, R.P. Rhoads, and L.H. Baumgard. 2015. Effects of in utero heat stress on

postnatal body composition in pigs: II. Finishing phase. J. Anim. Sci. 93(1):82–92. doi:10.2527/jas.2014–8355

Johnson, J.S., A. Sapkota, and D.C. Lay. 2016. Rapid cooling after acute hyperthermia alters intestinal morphology and increases the systemic inflammatory response in pigs. J. Appl. Physiol. 120(10):1249. doi:10.1152/japplphysiol.00685.2015

Kanehisa, M., M. Furumichi, M. Tanabe, Y. Sato, and K. Morishima. 2017. KEGG: new perspectives on genomes, pathways, diseases and drugs. Nucleic Acids Res. 45(Database issue):D353–D361. doi:10.1093/nar/gkw1092

Kim, J.K., J.J. Fillmore, M.J. Sunshine, B. Albrecht, T. Higashimori, D.W. Kim, Z.X. Liu, T.J. Soos, G.W. Cline, W.R. O'Brien, D.R. Littman, and G.I. Shulman. 2004. PKC-θ knockout mice are protected from fat-induced insulin resistance. J. Clin. Invest. 114(6):823–827. doi:10.1172/jci22230

Kotani, K., W. Ogawa, M. Matsumoto, T. Kitamura, H. Sakaue, Y. Hino, K. Miyake, W. Sano, K. Akimoto, S. Ohno, and M. Kasuga. 1998. Requirement of atypical protein kinase Cλ for insulin stimulation of glucose uptake but not for akt activation in 3T3-L1 adipocytes. Mol. Cell. Biol. 18(12):6971–6982. doi:10.1128/mcb.18.12.6971

Kregel, K.C. 2002. Invited review: heat shock proteins: modifying factors in physiological stress responses and acquired thermotolerance. J. Appl. Physiol. 92(5):2177. doi:10.1152/japplphysiol.01267.2001

Kuo, Y.-C., K.-Y. Huang, C.-H. Yang, Y.-S. Yang, W.-Y. Lee, and C.-W. Chiang. 2008. Regulation of phosphorylation of Thr-308 of Akt, cell proliferation, and survival by the B55α regulatory subunit targeting of the protein phosphatase 2A holoenzyme to Akt. J. Biol. Chem. 283(4):1882–1892. doi:10.1074/jbc.M709585200

Le Good, J.A., W.H. Ziegler, D.B. Parekh, D.R. Alessi, P. Cohen, and P.J. Parker. 1998. Protein kinase C isotypes controlled by phosphoinositide 3-kinase through the protein kinase PDK1. Science 281(5385):2042. doi:10.1126/science.281.5385.2042

Madhunapantula, S.V., and G.P. Robertson. 2011. Therapeutic implications of targeting AKT signaling in melanoma. Enzyme Res. 2011:327923. doi:10.4061/2011/327923

Marder, J., U. Eylath, E. Moskovitz, and R. Sharir. 1990. The effect of heat exposure on blood chemistry of the hyperthermic rabbit. Comp. Biochem. Physiol. A Physiol. 97(2):245–247. doi:10.1016/0300-9629(90)90179-V

Moeschel, K., A. Beck, C. Weigert, R. Lammers, H. Kalbacher, W. Voelter, E.D. Schleicher, H.-U. Häring, and R. Lehmann. 2004. Protein Kinase C-ζ-induced Phosphorylation of Ser318 in insulin receptor substrate-1 (IRS-1) attenuates the interaction with the insulin receptor and the tyrosine phosphorylation of IRS-1. J. Biol. Chem. 279(24):25157–25163. doi:10.1074/jbc.M402477200

Montilla, S.I.R., T.P. Johnson, S.C. Pearce, D. Gardan-Salmon, N.K. Gabler, J.W. Ross, R.P. Rhoads, L.H. Baumgard, S.M. Lonergan, and J.T. Selsby. 2014. Heat stress causes oxidative stress but not inflammatory signaling in porcine skeletal muscle. Temperature 1(1):42–50. doi:10.4161/temp.28844

Oehler-Jänne, C., A.O.V. Bueren, V. Vuong, A. Hollenstein, M.A. Grotzer, and M. Pruschy. 2008. Temperature sensitivity of phospho-Ser473-PKB/AKT. Biochem. Biophys. Res. Commun. 375(3):399–404. doi:10.1016/j.bbrc.2008.08.035

Pearce, S.C., S.M. Lonergan, E. Huff-Lonergan, L.H. Baumgard, and N.K. Gabler. 2015a. Acute heat stress and reduced nutrient intake alter intestinal proteomic profile and gene expression in pigs. PloS one 10(11):e0143099. doi:10.1371/journal.pone.0143099

Pearce, S.C., V. Mani, R.L. Boddicker, J.S. Johnson, T.E. Weber, J.W. Ross, R.P. Rhoads, L.H. Baumgard, and N.K. Gabler. 2013. Heat stress reduces intestinal barrier integrity and favors intestinal glucose transport in growing pigs. PloS one 8(8):e70215. doi:10.1371/journal.pone.0070215

Pearce, S.C., M.V. Sanz-Fernandez, J. Torrison, M.E. Wilson, L.H. Baumgard, and N.K. Gabler. 2015b. Dietary organic zinc attenuates heat-stress induced changes in pig intestinal integrity and metabolism. Journal of Animal Science 93(10):4702–4713. doi:10.2527/jas.2015-9018

Prunier, A., M.M. de Bragança, and J. Le Dividich. 1997. Influence of high ambient temperature on performance of reproductive sows. Livest Prod Sci 52(2):123–133. doi:10.1016/S0301-6226(97)00137-1

Ravichandran, L.V., D.L. Esposito, J. Chen, and M.J. Quon. 2000. PKC-ζ phosphorylates IRS-1 and impairs its ability to activate PI 3-kinase in response to insulin. J. Biol. Chem. 276(5):3543–3549. doi:10.1074/jbc.M007231200

Sanz Fernandez, M.V., S.K. Stoakes, M. Abuajamieh, J.T. Seibert, J.S. Johnson, E.A. Horst, R.P. Rhoads, and L.H. Baumgard. 2015a. Heat stress increases insulin sensitivity in pigs. Physiol. Rep. 3(8):e12478. doi:10.14814/phy2.12478

Sanz Fernandez, V.M., J.S. Johnson, M. Abuajamieh, S.K. Stoakes, J.T. Seibert, L. Cox, S. Kahl, T.H. Elsasser, J.W. Ross, S.C. Isom, R.P. Rhoads, and L.H. Baumga rd. 2015b. Effects of heat stress on carbohydrate and lipid metabolism in growing pigs. Physiological Reports 3(2):e12315. doi:10.14814/phy2.12315

Schmitz-Peiffer, C., and T.J. Biden. 2008. Protein kinase C function in muscle, liver, and β-cells and its therapeutic implications for type 2 diabetes. Diabetes 57(7):1774–1783. doi:10.2337/db07-1769

Shwartz, G., M.L. Rhoads, M.J. VanBaale, R.P. Rhoads, and L.H. Baumgard. 2009. Effects of a supplemental yeast culture on heat-stressed lactating Holstein cows1. J. Dairy Sci. 92(3):935–942. doi:10.3168/jds.2008-1496

Spitzer, J.A., and I.V. Deaciuc. 1992. Protein kinase C activity and lipogenesis from glucose in isolated adipocytes of endotoxemic rats. Circ. Shock 37(2):111–116.

St-Pierre, N.R., B. Cobanov, and G. Schnitkey. 2003. Economic losses from heat stress by US livestock industries1. J. Dairy Sci. 86, Supplement(0):E52–E77. doi:10.3168/jds.S0022-0302(03)74040–5

Standaert, M.L., L. Galloway, P. Karnam, G. Bandyopadhyay, J. Moscat, and R.V. Farese. 1997. Protein kinase C-ζ as a downstream effector of phosphatidylinositol 3-kinase during insulin stimulation in rat adipocytes: potential role in glucose transport. J Biol Chem. 272(48):30075–30082. doi:10.1074/jbc.272.48.30075

Temim, S., A.-M. Chagneau, R. Peresson, and S. Tesseraud. 2000. Chronic heat exposure alters protein turnover of three different skeletal muscles in finishing broiler chickens fed 20 or 25% protein diets. J. Nutr. 130(4):813–819.

Tobias, I.S., M. Kaulich, P.K. Kim, N. Simon, E. Jacinto, S.F. Dowdy, C.C. King, and A.C. Newton. 2016. Protein kinase Cζ exhibits constitutive phosphorylation and phosphatidylinositol-3,4,5-triphosphate-independent regulation. Biochem. J. 473(4):509–523. doi:10.1042/bj20151013

Tremblay, F., C. Lavigne, H. Jacques, and A. Marette. 2001. Defective insulin-induced GLUT4 translocation in skeletal muscle of high fat–fed rats is associated with alterations in both Akt/protein kinase B and atypical protein kinase C (ζ/λ) activities. Diabetes 50(8):1901–1910. doi:10.2337/diabetes.50.8.1901

Vicario, S.J., R. Okabajue, and T. Haltom. 1986. Rapid cooling in classic heatstroke: effect on mortality rates. Am. J. Emerg. Med. 4(5):394–398. doi:10.1016/0735-6757(86)90185-3

Vivanco, I., and C.L. Sawyers. 2002. The phosphatidylinositol 3-Kinase-AKT pathway in human cancer. Nat. Rev. Cancer 2(7):489–501. doi:10.1038/nrc839

Wang, X., and C.G. Proud. 2006. The mTOR pathway in the control of protein synthesis. Physiology 21(5):362–369. doi:10.1152/physiol.00024.2006

Wheelock, J.B., R.P. Rhoads, M.J. VanBaale, S.R. Sanders, and L.H. Baumgard. 2010. Effects of heat stress on energetic metabolism in lactating Holstein cows1. J. Dairy Sci. 93(2):644–655. doi:10.3168/jds.2009–2295

Xia, J., I.V. Sinelnikov, B. Han, and D.S. Wishart. 2015. MetaboAnalyst 3.0—making metabolomics more meaningful. Nucleic Acids Res. 43(Web Server issue):W251–W257. doi:10.1093/nar/gkv380

Xu, N., Y. Lao, Y. Zhang, and D.A. Gillespie. 2012. Akt: a double-edged sword in cell proliferation and genome stability. J. Oncol. 2012:951724. doi:10.1155/2012/951724

Yunianto, V.D., K. Hayashi, S. Kaneda, A. Ohtsuka, and Y. Tomita. 1997. Effect of environmental temperature on muscle protein turnover and heat production in tube-fed broiler chickens. Br. J. Nutr. 77(6):897–909.

Zhang, Z.Y., G.Q. Jia, J.J. Zuo, Y. Zhang, J. Lei, L. Ren, and D.Y. Feng. 2012. Effects of constant and cyclic heat stress on muscle metabolism and meat quality of broiler breast fillet and thigh meat. Poult. Sci. 91(11):2931–2937. doi:10.3382/ps.2012–02255